International Journal Of
Industrial Electronics Control and Optimization
Print ISSN: 3517-2645
Online ISSN: 3568-2645
Homepage: https://ieco.usb.ac.ir/

Dynamic Multi-Level Generation and Transmission Expansion Planning Model of Multi-Carrier Energy System to Improve Resilience of Power System

Mahnaz Rezaei[1] | Mohammad Tolou Askari[2] | Meysam Amirahmahdi[3] | Vahid Ghods[4]

Department of Electrical Engineering, Semnan Branch, Islamic Azad University, Semnan, Iran.[1,2,3,4]
Corresponding author's email: m.askari@semnaniau.ac.ir

Article Info

Article type:
Research Article

Article history:
Received: 2022-May-13
Received in revised form: 2022-Nov-11
Accepted: 2023-Jan-08
Published online: 2023-Feb-19

Keywords:
Corrective actions,
Coordinated GEP & TEP,
Multi-Carrier energy system,
Resilience improvement

ABSTRACT

Recently, natural disasters such as earthquakes have threatened the power system resilience. On the other hand, the effect of sudden disruptions on equipment, demand growth, shortage of energy resources and high cost of power system expansion have necessitated special attention to demand response programs (DR) and considering uncertainties. Since the presence of an energy hub (EH) leads to change the expansion planning problem of electrical power system. Therefore, in this study, the nature of optimal generation and transmission expansion planning in the presence of EH is studied. Also, the effect of applying the proposed hub with and without considering energy storages (ESs) as well as the short and long-term corrective actions to reduce the losses and costs are investigated. In addition, demand response and line transmission switching are considered as effective approaches to improve resilience in the proposed dynamic multi-level model. This nonlinear problem is solved sequentially considering the random approach and using differential evolution algorithm (DEA) and the symphony orchestra search algorithm (SOSA). In this paper, the proposed objective functions are studied in five-level and the results show the efficiency of this model in solving the planning problem. The findings show that the proposed planning model decreased capital costs of transmission switches as much as 26%, the capital cost of the transmission as much as 2.29%, the congestion cost as much as 1.8%, The capital cost of generation units as much as 3.75%, the payment capacity paid to generation units as much as 1.8%. Also, the expected profit of the generation units has increased as much as 3.75%. To show the competence of the proposed algorithms, the 400-kV test system with 52 buses in Iran is simulated in MATLAB environment

NOMENCLATURE

Sets:

x. *X*	decision making variables of the corrective actions.
t, T	Time (hour).
a, A	Installed generating units.
d, D	Existing generating units.
i, I	Suppliers.
j, J	Consumers.
p, P	Patterns.
r, R	Earthquakes scenarios.
c, C	Attacks scenarios.
n, N	Intensities of event.
w, W	Scenarios for ruining the GenCos and transmission lines in *r* with severity *n*.
h, H	Earthquake –prone geographical regions.
e, E	Load sectors on each load bus.
b, B	Buses.
gu, GU	Decision making variables of the GEP problem.
z, Z	Decision making variables of the events problem.

NOMENCLATURE -CONTINUED

tl, TL	Corridors.
Constant Parameters:	
$D_{t,p,u,e}^{max}$	Maximum annual load demand at sector e of bus u.
FCC_{TL}	Construction cost for a transmission line.
FCC_{TS}	Construction cost for a transmission switch.
$G_{t,p,i}^{min} G_{t,p,i}^{ma}$	Lower and upper bounds of production of GenCo i.
FIC_{t,i_a}^{nG}	Fixed investment cost for the installed generating unit.
π_E^{WIND}	Operation cost wind turbine.
L_{tl}	Length of corridor.
$EENS^{max}$	Maximum value of the expected energy not supplied.
$\mathrm{IC}^{\mathrm{EENS}}$	Cost of expected energy not supplied.
RM_t^{max} ,	Lower and upper limits for reserve margin.
t_0	Base year.
TL^{max}	Maximum number of transmission lines augmented in corridor.
CF^g	Corrective factor related to the reliability.
σ_{t,p,i_a}^{nG}	Constant coefficients of the apparent production cost.
$\Gamma^{r(n):w(h)}$	Outage duration events.
$D_{t,p,j}^{min}$, D_t^{l}	Lower and upper limits consumption of DisCo.
$\omega_{t,p,u,e}^{r(n):w(h)}$	Weight coefficient of load curtailment at sector e.
Decision Variables:	
$EENS_t$	Expected energy not supplied.
TL	Transmission lines augmented in corridor.
TS	Transmission switches augmented in corridor.
$D_{t,p,j}^{r(n):w(h)}$	Consumption of DisCo.
CC_{total}	Total congestion cost.
$CAP_{t,i}^{Gu}$	Capacity payment the generation units.
CAP_{t,p,i_d}^{eG}	Capacity of existing generating unit.
$EB_{t,i}^{Gu}$	Expected profit the generation units.
EB_{t,i_a}^{nGu}	Expected profit the candidate installed generation unit.
IC_{t,i_a}^{nGu}	Capital cost the candidate installed generating units.
$F_{t,tl}$	Active power flow in corridor.
P_H^{ch}, P_H^{dis}	Amount charging and discharging thermal storage.
$G_{t,p,i}^{r(n):w(h)}$	Production of GenCo i.
D_{peak}	Average peak demand.
CAP_{t,i_a}^{nG}	Installed Capacity of the new generating units.
IC_t^{TL}	Capital cost candidate installed transmission lines.
$IC_{t,tl}^{TS}$	Capital cost candidate installed transmission switch.
VIC_{t,i_a}^{nG}	Variable investment cost the installed generating unit.
$\chi_{t,p,u,e}^{r(n):w(h)}$	Amount of curtailed load at sector e of bus u.
$\vartheta_{t,p,u,i_a}^{nG}$	Predicted market price the candidate installed generating unit.
$\theta_{t,p,v}^{r(n):w(h)}$	Phase angle on the receiving bus of corridor.
$\theta_{t,p,u}^{r(n):w(h)}$	Phase angle on the sending bus of corridor.
θ_α , θ_β	Voltage angles of the node α , β.
δ_{t,p,i_a}	Expected power not supplied before installation of new generating unit.
$Y_{t,p,tl}^{r(n):w(h)}$	Element at the u row and v column in the admittance matrix.

I. Introduction

Power network is one of the most complex networks of the world, and recently has the study of the term "resilience" is one of the main keywords of the power system among industry and academic sectors. Resilience, indicates the capability of an entity or system to recover its normal condition in the shortest time after a failure that changes the system state. In order to guarantee the security plus reliability of the power system, research related to GTEP with the integration of renewable energy systems (RESs) is of great significance. On the other hand, energy hub systems (EHSs) are fully in line with the

future policies of sustainable cities and society [1]. Therefore, with the coordinated use of different infrastructures to meet the needs of customers with increased efficiency, reducing losses, reducing emissions and operating costs, we can see the improvement of this criteria [2]. Considering that climate changes increasing in recent years, natural disasters such as earthquakes and etc can lead to significant losses. Power outages affected more than 710,000 customers in 2015 due to Canada's windstorm, and 1.7 million customers in 2016 due to a massive flood in Australia [3]. The failure of Beijing's transportation system in 2016 due to heavy rains canceled hundreds of flights and trains [4]. Hurricanes cut off more than 7 million customers in Florida, Georgia and South Carolina in 2017, and Hurricane Harvey, which occurred at the same year, resulted in power outage of more than 2 million customers [5]. Since natural disasters affect devices, especially worn-out devices, and constructing more powerful devices is not cost-effective, an efficient planning to heighten power system resilience might be useful. Various studies have discussed the certain and random expansion planning models either in static form or in multiple steps [6]. In [7], expansion planning has been presented to increase resilience in the presence of hybrid micro grids, and a strategy has been formulated to minimize load curtailment and a resilience index has been presented to evaluate performance of the proposed strategy during emergency operations.

In [8], the optimization of integrated generation and transmission expansion is dealt with in the US in a time frame extending to 2050. In [9], a stochastic optimal transmission switching (SOTS) model is developed considering the uncertainty of load, wind power and photovoltaic generation, while minimizing the grid vulnerability. Scenario reduction technique is used for alleviating computational burden of the developed SOTS model. The authors of [10], have solved the GTEP problem considering a random approach that only considers uncertainties. This problem is applied to a power system that is similar to a real system and considers renewable energy resources (wind energy farms) for probabilistic integration. In [11], CGTEP has been presented considering environmental pollution and reliability in the presence of wind turbine and FACTS. In [12], presents a multi-objective bi-level model for planning and operation of integrated energy systems considering the DR program.

In [13], presents a multi-objective optimization framework for long-term planning of EH, in which equipment degradation and integrated demand response (IDR) programs are considered. In [14], proposes a coordinated planning method of power systems and energy transportation networks (ETNs) for resilience enhancement. The uncertainty that occurred due to extreme events such as the use of conventional state-attack has been considered. In [15], a vulnerability-constrained model has been given for the CGTEP considering seismic- and terrorist-induced events. In [16], a plan consisting of investment and operation method has been proposed for controlling the resilience of coupled power distribution and transportation systems. In [17], a model has been proposed that integrates the arranging of the repair sequence of injured components. In [18], a three-level model has been proposed for the sizing problem of networked MGs.

This model solves the problem optimally and considered resilience and cost. In [19], the scenario-based technique has been used to incorporate three dissimilar conditions i.e. daytime with clear-sky and no-fault, daytime with abnormal events, and nighttime into the stochastic dynamic optimization problem for co-existence of PV plants and the load in a service area. Furthermore, the risk-constrained stochastic dynamic SEP problem and Mixed Integer Linear Programming (MILP) framework for one roof has been combined in this reference. In [20], a fragile model is established for investigating the nodal SCF probability.

In this model, the insulation aging of equipment and extreme weather events has been considered. Then, to show the cascading effects of expected SCFs, a response framework for extreme weather conditions is established for a transmission system. In [21], an all-inclusive process has been suggested that helps the system operators to take good decisions for controlling power system resilience and economic value when a severe weather event occurs. In [22], with the help of ensemble numerical weather forecasts a decision-making model for unit scheduling has been suggested. Since the determining the best transmission line to switch by an appropriate time is the main problem for the applicability of TS in wider range. In [23], a heuristic transmission switching (TS) algorithm has been given for increasing resilience by decreasing the load shed in electricity networks affected by extreme weather events (EWEs).

This presented algorithm is fast and scalable. In [24], a transmission resilience planning solution has been suggested by defining the lines to be placed underground for minimizing load shedding in the most cost-efficient method considering historical EWEs (HEWEs). This phenomenon has been considered as a stochastic robust optimization problem and the worst damage situation by the objective function of maximizing load shedding. In [25], a probabilistic proactive generation redispatch strategy has been presented to improve the operational resilience of power grids through wildfires. In [26], a proactive generation redispatch strategy has been proposed to improve the operational resilience of power grids through hurricanes regarding inaccessibility and forced disconnection of renewable energy sources (RESs). The presented results confirm the proactive and dynamic

generation redispatch is effective in improving power system resilience and capability.

This generation redispatch decreases the load curtailments with restricted generation resources through hurricanes by at least 40%. In [27], a two-stage stochastic planning model has been proposed for transmission systems and distributed energy resources (DERs). In this model, the resiliency of the power system has been considered. Furthermore, the normal and emergency situations and their event time has been taken into account. In [28], to determine the probability of failure events, the failure rates of transmission lines due to extreme weather conditions have been modeled.

Then, to schedule generators, optimally and flexible loads while meeting the frequency security restrictions under transmission line failure events, a two-stage stochastic frequency constrained unit commitment (FCUC) model is presented. In [29], a resiliency investment optimization model has been suggested that defines optimal investments in the transmission grid for protecting against extreme weather events. This model consists of OTS and generator dispatch decisions for minimizing unserved load through an extreme weather event. In [30], a static model for coordinated generation and transmission expansion planning (CGTEP) has been presented. This model alleviate the vulnerability of power system in contrast to physical deliberate attacks in the horizon of planning. In addition, the physical deliberate attacks and their subsequent influences are evaluated through the process of scenario building. In [31], the capacity expansion and switch installation in electric systems has been combined which results in optimum performance during nominal operations and attacks. This model provides bridges long-term system planning for transmission development and short-term switching operations response to attacks. In [32], the vulnerability of the power system exposed to physical deliberate attacks (PDAs) has been investigated while the power system and communication network are geographic-cyber codependents. The attacker applies a PDA on transmission lines and the communication network to injure the power system, and on the other side, the system operator (SO) reacts as a defender by doing essential actions against them.

The following gaps are reported base on the literature review.

- The coordination GEP and TEP to improve the resilience was ignored.
- Effects of multi-carrier energy system in CGTEP was ignored.
- The natural disaster such as earthquake was not considered in the previous studies.
- Finally, a dynamic and comprehensive model by considering DR, ES, uncertainties, RES, and corrective actions were not given in the previous researches.

The novelties of this paper are compared with recent works and is shown in Table 1.

The main contributions of this paper are as follows:

- To provide an improved dynamic model, coordinated GTEP by applying the proposed hub, wind turbine, and electrical and thermal storage.
- To develop a new five-level architecture using short and long-term corrective actions on three scales by considering DR programs, uncertainties, social welfare, reliability to improve the resilience in the power system.
- To develop the model by considering the proposed EH.
- To investigate random scenarios to reach an overall optimal point and to solve the proposed large-scale mixed integer nonlinear five-level model with the aim of strengthening the resilience of power systems, which has been considered in limited studies in the field of generation and transmission expansion planning.

The rest of this article is organized as follows: Section 2 formulates the proposed model, objective function and constraints of different levels. Section 3 describes the proposed model solution using mathematical algorithms. Section 4 presents the numerical results and the calculation on the 52-bus network in Iran. Finally, conclusions are explained in Section 5.

TABLE 1
COMPARISON OF THIS PAPER WITH RECENT PUBLISHED PAPERS

Ref	Objective function	CGTEP	Implementation approach	Muiti-level model	Type event	Vulnerability assessment	transmission switching	Renewable	Uncertainty	ES	DR program	Resilience
[2]	Cost & Loss & Emission	×	MILP CPLEX solver	×	Seasonal variation	×	×	✓	✓	✓	✓	✓
[9]	Cost	×	MINLP	×	×	✓	✓	✓	✓	×	×	×
[10]	Cost	×	MILP	×	×	×	✓	✓	✓	×	×	×
[11]	Cost & Profit & Emission	✓	MINLP	×	×	×	×	✓	✓	×	×	×
[12]	Cost & Profit & Emission	×	NSGA-II algorithm	Bi-level	×	×	×	✓	✓	✓	✓	×
[13]	Cost & Loss & Emission	×	Max-min fuzzy method	×	×	×	×	✓	✓	✓	✓	×
[14]	Cost	×	Two stage robust programming	Tri-level	×	×	×	✓	✓	×	×	✓
[15]	Cost & Profit & Loss	✓	MINLP&SOS algorithm	Quad-level	Seismic-terrorist	✓	✓	×	✓	×	✓	✓
[16]	Cost	×	Benders decomposition and C&CG algorithms	Tri-level	Natural disaster	×	✓	×	✓	×	×	✓
[17]	Cost	×	p-robust & scenario-based decomposition	×	attack	×	×	×	✓	×	×	✓
[18]	Cost	×	AG algorithm	Tri-level	Damage system	×	×	✓	✓	×	×	✓
[19]	Cost	×	MILP	×	×	×	×	✓	✓	×	✓	✓
[20]	Cost	×	MINLP	×	×	×	✓	×	✓	×	×	✓
[21]	Cost & Profit	×	Decision analysis	×	Typhoon	×	×	✓	✓	×	×	✓
[22]	Cost	×	Decision making	×	Typhoon	×	×	✓	✓	×	×	✓
[23]	Cost	×	MIP TS algorithm	×	Typhoon	×	✓	×	×	×	×	✓
[24]	Cost	×	Decomposition-based algorithm & Monte Carlo	×	Natural disaster	✓	×	×	✓	×	×	✓
[25]	Cost	×	Markov decision CPLEX solver	×	wildfires	×	×	×	✓	×	×	✓
[26]	Cost	×	MILP	×	Typhoon	×	×	✓	✓	×	×	✓
[27]	Cost	×	MILP Benders decomposition technique	Bi-level	Emergency condition	✓	×	×	✓	×	×	✓
[28]	Cost	×	regularized L-shape algorithm	×	extreme weather	×	×	×	✓	×	×	✓
[29]	Cost	×	SOCP programming	×	Typhoon	×	✓	✓	✓	×	×	✓
[30]	Cost	✓	MILP CPLEX solver	Bi-level	attack	✓	×	×	✓	×	×	×
[31]	Cost	×	MIP decomposition via two-layer cutting plane algorithm	Tri-level	attack	×	✓	✓	✓	×	×	✓
[32]	Cost	×	MILP-genetic algorithm CPLEX solver	Bi-level	attack	✓	×	×	✓	×	×	×
This paper	Cost & Profit & Loss	✓	MINLP DE algorithm &SOSA	Five-level	Earthquake	✓	✓	✓	✓	✓	✓	✓

II. Proposed model of multi period CGTEP problem

Recently, various challenges in the context of power system resilience have concerned the researchers [33]. On the other hand, simultaneous operation of different generation and transmission infrastructures like artificial electricity and gas network has been presented under the concept of EH, which is cost-effective to be employed for heightening resilience. In this study, the EH includes boiler, CHP, transformer, converters, and wind turbine. The network inputs include gas, electricity and heat, that enter the network, and the network outputs include electricity and heat. The schematic of a multi-carrier energy system that operates as an interface between input and output energy carriers is shown in Fig. 1.

A. First Level Planning

The objective function at the first level includes operational costs and input energy transmission costs. In this study, the input carriers include electricity, natural gas, heat, energy storage systems, and wind turbine, which are described in Equ. (1) [34].

$$\min F = \sum_{t=1}^{24} IC_E(t)+IC_G(t)+IC_H(t)+IC_{ES}(t)+IC_{HS}(t) \quad (1)$$

In the first level objective function, IC_E is the cost of electricity transmission (including the electricity transmission cost from wind turbines and the electricity transmission cost from the electricity market); IC_G, IC_H, IC_{ES}, and IC_{HS} are the costs of natural gas, heat transmission, electrical and thermal energy storage system which are described using Equs. (2)-(6).

$$IC_E(t)=\left[\pi_E^{NET}(t)P_E^{NET}(t)\right]+\left[\pi_E^{WIND}(t)P_E^{WIND}(t)\right] \quad (2)$$

$$IC_G(t)=\left[\pi_G^{NET}(t)P_G^{NET}(t)\right] \quad (3)$$

$$IC_H(t)=\left[\pi_H^{NET}(t)P_H^{NET}(t)\right] \quad (4)$$

$$IC_{ES}(t)=\left[\pi_E^{op}\left(P_E^{ch}(t)+P_E^{dis}(t)\right)\right]+\left[\pi_E^{NET}(t)\left(P_E^{ch}(t)-P_E^{dis}(t)\right)\right] \quad (5)$$

$$IC_{HS}(t)=\left[\pi_H^{op}\left(P_H^{ch}(t)+P_H^{dis}(t)\right)\right]+\left[\pi_H^{NET}(t)\left(P_H^{ch}(t)-P_H^{dis}(t)\right)\right] \quad (6)$$

where π_E^{NET}, π_E^{WIND}, π_G^{NET}, and π_H^{NET} are the cost of purchasing each kWh of power from the grid, wind turbine, gas and heat network at time *t*, respectively; π_E^{op} and π_H^{op} are the operation cost of electrical and thermal energy, respectively; P_E^{NET}, P_E^{WIND}, P_G^{NET}, and P_H^{NET} represent the electrical power of the grid, wind turbine, natural gas power taken from the network and the input thermal power of the network, respectively; P_E^{ch}, P_E^{dis}, P_H^{ch}, and P_H^{dis} are the amount of power (charge-discharge) of the electrical and thermal energy storage systems, respectively.

1) First Level Planning Constraints

All devices of the EHS have constraints like limited output power, and etc. These constraints along with power generation and consumption balance are described in this section. Equ. (7) represents the electrical energy balance in the EH that sets the generated electricity power equal to the demanded electricity power.

$$P_E^D(t)=\left\{\begin{array}{l}\left[\eta_E^T P_E^{NET}(t)\right]+\left[\eta_{GE}^{CHP} P_G^{NET\,CHP}(t)\right]+\\ \left[\eta_{CONV}^{WIND} P_E^{WIND}(t)\right]+\left[P_E^{dis}(t)-P_E^{ch}(t)\right]\end{array}\right\} \quad (7)$$

In Equ. (7), η_E^T, η_{CONV}^{WIND}, and η_{GE}^{CHP} represent the electric transformer coefficient, the wind turbine converter efficiency, the CHP system efficiency to convert the input gas power into electric power respectively; Equ. (8) represents the balance of the input and output gas of the EH [34].

$$P_G^D(t)=P_G^{NET}(t)-P_G^{NET\,CHP}(t)-P_G^{NET\,BOIL}(t) \quad (8)$$

where P_G^{NETCHP} and $P_G^{NETBOIL}$ are the natural gas power received from the CHP and boiler system, respectively; The heat demand is the amount of thermal energy used to heat the consumption water in the central heating system, as given:

$$P_H^D(t)=\left\{\begin{array}{l}\left[\eta_{GH}^{CHP} P_G^{NET\,CHP}(t)\right]+\left[\eta_{GH}^{BOIL} P_G^{NET\,BOIL}(t)\right]\\ +\left[P_H^{dis}(t)-P_H^{ch}(t)\right]+P_{BOIL}^{NET}(t)\end{array}\right\} \quad (9)$$

In Equ. (9), η_{GH}^{BOIL} and η_{GH}^{CHP} represent the efficiency of the boiler and the CHP system for converting gas to heat, respectively. Since the network generation has a certain capacity, and it cannot be operated more than its capacity, the network power limits are expressed in Equs. (10)-(13) [34].

$$0 \le P_E^{NET}(t) \le P_E^{NET\,MAX} \quad (10)$$

$$0 \le P_E^{NET}(t) \le P_{IN}^{T} \quad (11)$$

$$0 \le P_G^{NET\,CHP}(t) \le P_{IN}^{CHP} \quad (12)$$

$$0 \le P_G^{NET\,BOIL}(t) \le P_{IN}^{BOIL} \quad (13)$$

where $P_E^{NET\ MAX}$, P_{IN}^{BOIL}, P_{IN}^{CHP}, and P_{IN}^{T} represent the maximum power capacity received from the network, the maximum capacity of CHP, and the maximum capacity of electrical transformers. The output power of the wind turbine depends on the wind speed, and varies regarding the turbine speed as given in the following equation [34]:

$$P_E^{WIND}(v(t))=\left\{\begin{array}{ll}0 & ;v(t)\le v_{in}\ge v_{out}\\ \dfrac{v(t)-v_{in}}{v_r-v_{in}}P_r^{WIND} & ;v_{in}\le v(t)\le v_r\\ P_r^{WIND} & ;v_r\le v(t)\ge v_{out}\end{array}\right\} \quad (14)$$

2) DS-DOCR Characteristics

In (1), the formula for standard relay tripping time is shown. As seen, the tripping time of DOCRs is a function of the short-circuit current that passes the relays. In addition, the coefficients for standard characteristics are given in Table 2 [4, 12].

$$t_i = TDS_i \frac{A_i}{\left(\frac{I_{F,i}}{I_{p,i}}\right)^{B_i} - 1} \quad (15)$$

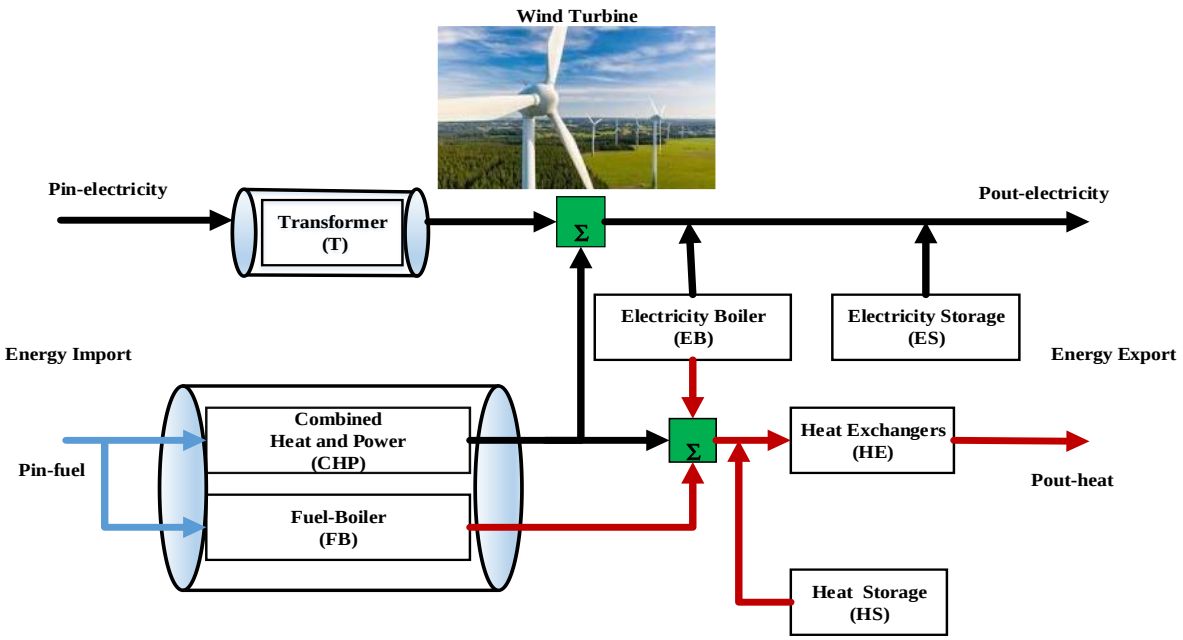

Fig. 1. Structure energy hub system.

In Equ. (14), P_r^{WIND} and v_r represent the rated speed and rated output power of wind turbine respectively; $v(t)$ represent the wind speed at time t and scenario s. v_{in} and v_{out} , represent the cut in and cut out speeds of wind turbine, respectively.

B. Second Level Planning

At this level, first the purpose is to consider corrective actions like network re-generation and reconfiguration to minimize technical and economic losses, maximize social welfare and minimize load curtailment. the second level objective function is described using Equ. (16) [15], [35]:

$$\max_{x\in X} \mathbf{of:} OF = \begin{bmatrix} \sum_{j\in J} \sigma_{t,p,j} \left(\left(D_{t,p,j}^{r(n):w(h)} \right)^2 + D_{t,p,j}^{r(n):w(h)} + 1 \right) - \\ \sum_{i\in I} \sigma_{t,p,i} \left(\left(G_{t,p,i}^{r(n):w(h)} \right)^2 + G_{t,p,i}^{r(n):w(h)} + 1 \right) - \\ \sum_{u\in B} \sum_{e\in E} \chi_{t,p,u,e}^{r(n):w(h)} . IC_{t,p,u,e}^{r(n):w(h)} \left(\Gamma^{r(n):w(h)} \right) \omega_{t,p,u,e}^{r(n):w(h)} \end{bmatrix} \quad (16)$$

where $\sigma_{t,p,j}$ and $\sigma_{t,p,i}$ are the significant profit coefficients of Disco j consumer and GenCo i generation cost, respectively; $D_{t,p,j}^{r(n):w(h)}$ and $G_{t,p,i}^{r(n):w(h)}$ are the consumption of Disco j and generation of GenCo i, respectively; $\chi_{t,p,u,e}^{r(n):w(h)}$ is the load curtailment rate. $IC_{t,p,u,e}^{r(n):w(h)}(\Gamma^{r(n):w(h)})$ is the load curtailment cost over time resulting from disasters and $\omega_{t,p,u,e}^{r(n):w(h)}$ is the load curtailment weight coefficient.

1) Second Level Planning Constraints

In this section, described network balance in which $D_{t,p,j,u,e}^{max}$ is the maximum annual load demand, $Y_{t,p,tl}^{r(n):w(h)}$ represents the elements of the network admittance matrix, and $\theta_{t,p,v}^{r(n):w(h)}$ represents the received bus phase angle in Equ. (17) [15].

$$G_{t,p,i,\mu}^{r(n):w(h)} - \sum_{e\in E} \left(D_{t,p,j,\mu,e}^{max} - \chi_{t,p,\mu,e}^{r(n):w(h)} \right) = \sum_{tl\in L} Y_{t,p,tl}^{r(n):w(h)} \theta_{t,p,v}^{r(n):w(h)} \quad (17)$$

Equ. (17) is the limit of power generated by each GenCo i, and Equ. (18) shows the power purchased by each DisCo j, where $G_{t,p,i}^{max}$ and $G_{t,p,i}^{min}$ are the upper and lower limits of GenCo i generation, also $D_{t,p,j}^{max}$ and $D_{t,p,j}^{min}$ are the upper and lower limits of Disco j consumption [17].

$$G_{t,p,i}^{min} \le G_{t,p,i}^{r(n):w(h)} \le G_{t,p,i}^{max} \quad (18)$$

$$D_{t,p,j}^{min} \le D_{t,p,j}^{r(n):w(h)} \le D_{t,p,j}^{max} \quad (19)$$

Equ. (20) shows the allowed amount of load curtailment at different accident severity scales:

$$\chi_{t,p,u,e}^{r(n):w(h)} \le D_{t,p,u,e}^{max} \quad (20)$$

The power flow relationship of the transmission line and its safety constraints are formulated in Equs. (21)-(23) which the power flow is represented by $F_{t,p,tl}^{r(n):w(h)}$. $F_{t,p,tl}^{max}$ is the maximum active power flow [15].

$$F_{t,p,tl}^{r(n):w(h)} - Y_{t,p,tl}^{r(n):w(h)} \left(\theta_{t,p,u}^{r(n):w(h)} - \theta_{t,p,v}^{r(n):w(h)} \right) = 0 \tag{21}$$

$$-\left| Y_{t,p,tl}^{r(n):w(h)} \cdot \left(\theta_{t,p,u}^{r(n):w(h)} - \theta_{t,p,v}^{r(n):w(h)} \right) \right| \le F_{t,p,tl}^{\max} \tag{22}$$

$$-\left| Y_{t,p,tl}^{r(n):w(h)} \left(\theta_{t,p,v}^{r(n):w(h)} - \theta_{t,p,u}^{r(n):w(h)} \right) \right| \le F_{t,p,tl}^{\max} \tag{23}$$

C. Third level Planning

At this level, the technical and economic loss function is maximized regarding the accidents severity to maximize resilience of the generation and transmission networks [15].

$$\max_{z \in Z} \left[\sum_{b \in B} \sum_{e \in E} \chi_{t,p,u,e}^{r(n):w(h)} . \mathrm{IC}_{t,p,u,e}^{r(n):w(h)} \left(\Gamma^{r(n):w(h)} \right) \right] \tag{24}$$

1) Third Level Planning Constraints:

In this section, Limitations related to the transmission lines and generation units, that can be damaged during earthquake, are defined in Equs. (25)-(28).

$$\sum_{\forall i \in I} \varphi_{t,p,i}^{r(n):w(h)} \le \varphi_{i,\max}^{r(n)} \tag{25}$$

$$\sum_{\forall tl \in L} \varphi_{t,p,tl}^{r(n):w(h)} \le \varphi_{L,\max}^{r(n)} \tag{26}$$

$$\sum_{\forall i \in I} \varphi_{t,p,i}^{c(m):q(k)} \le \varphi_{i,max}^{c(m)} \tag{27}$$

$$\sum_{\forall tl \in L} \varphi_{t,p,tl}^{c(m):q(k)} \le \varphi_{L,\max}^{c(m)} \tag{28}$$

where $\varphi_{t,p,i}^{r(n):w(h)}$ is the number of generation units, and $\varphi_{t,p,tl}^{r(n):w(h)}$ is the number of transmission lines which might be destroyed in *r* with severity *n* under scenario *w* at earthquake-prone geographical area *h*, respectively; $\varphi_{t,p,i}^{c(m):q(k)}$ is the number of generation units, and $\varphi_{t,p,tl}^{c(m):q(k)}$ is the number of transmission lines which might be destroyed in *c* with severity *m* under scenario *q* at attack-prone geographical area *k*, respectively [15], [31], [32].

D. Fourth Level Planning

At this level, generation expansion planning is proposed to heighten resilience. In Equ. (29), $EB^{GU}{}_{t,i}$ represents the expected profit of the GenCo *i*, $IC_{t,i}^{nGU}$ represents the capital cost of the generation units associated with the new installation capacity by GenCo *i*. $CAP_{t,i}^{GU}$ represents the payment capacity paid by the generation units to heighten resilience [15].

$$\max_{gu \in GU} \text{of}: OF = \left[\sum_{t \in T} \frac{EB_{t,i}^{GU}}{(1+d)^{t-t_0}} - \sum_{t \in T} \frac{IC_{t,i}^{nGU}}{(1+d)^{t-t_0}} + \sum_{t \in T} CAP_{t,i}^{GU} \right] \tag{29}$$

The second term in Equ. (29) indicates the fixed and variable investment costs of each generation unit during the planning period, which is described as follows:

$$IC_{t,i_a}^{nGU} = VIC_{t,i_a}^{nG} + FIC_{t,i_a}^{nG} \tag{30}$$

In Equ. (30), the variable investment cost as the product of investment cost associated with each generation unit by the installation capacity of each generation unit, can be calculated using Equ. (31):

$$VIC_{t,i_a}^{nG} = IC_{t,i_a}^{G} \cdot CAP_{t,i_a}^{nG} \tag{31}$$

where IC_{t,i_a}^{G} is capital cost for generating unit; CAP_{t,i_a}^{nG} is installed capacity of candidate generating by Genco *i*. In Equ. (32), the expected profit is obtained using the total expected profit associated with the new and existing installed generation units as given [15]:

$$EB_{t,i}^{GU} = \sum_{a \in A} EB_{t,i_a}^{nGU} + \sum_{d \in D} EB_{t,i_d}^{eGU} \tag{32}$$

Equs. (33) and (34) describe the expected profit associated with each new and existing installed generation unit in which D_p is the period length, $\vartheta_{t,p,u,i_a}^{nG}$ and $\vartheta_{t,p,u,i_a}^{eG}$ are the predicted market price for installing new and existing generation units, respectively; CAP_{t,p,i_a}^{nG} and CAP_{t,p,i_d}^{eG} are the capacity of each new and installed generation unit with GenCo *i*, respectively.

$$EB_{t,i_a}^{nGU} = \sum_{p \in P} \sum_{a \in A} D_p \left[\vartheta_{t,p,u,i_a}^{nG} CAP_{t,p,i_a}^{nG} - \left(\sigma_{t,p,i_a}^{nG} \left(CAP_{t,p,i_a}^{nG} \right)^2 + CAP_{t,p,i_a}^{nG} + 1 \right) \right] \tag{33}$$

$$EB_{t,i_d}^{eGU} = \sum_{p \in P} \sum_{d \in D} D_p \left[\vartheta_{t,p,u,i_d}^{eG} CAP_{t,p,i_d}^{eG} - \left(\sigma_{t,p,i_d}^{eG} \left(CAP_{t,p,i_d}^{eG} \right)^2 + CAP_{t,p,i_d}^{eG} + 1 \right) \right] \tag{34}$$

The payment capacity paid by generation units to heighten resilience is given in Equ. (35). In this equation, δ_{t,p,i_a} and ρ_{t,p,i_a} are the expected power not supplied before and after installing each generation unit by GenCo *i*, respectively; and IC^{EENS} is the expected cost not supplied.

$$CAP_{t,i}^{GU} = \sum_{p \in P} \sum_{a \in A} D_p \left[\left(\delta_{t,p,i_a} - \rho_{t,p,i_a} \right) \left(IC^{EENS} - \vartheta_{t,p,u,i_a}^{nG} \right) \right] \tag{35}$$

1) Fourth Level Planning Constraints

In this section, the limitations associated with generation expansion planning, including the capacity of each installed new generation unit and the investment cost of each generation unit are described in Equs. (36)-(38) [15]:

$$0 \le CAP_{t,i_a}^{nG} \le CAP_{t,i_a}^{nG\max} \tag{36}$$

$$0 \le IC_{t,i_a}^{nG} \le IC_{t,i_a}^{nG\max} \tag{37}$$

$$G_{t,p,i}^{\min} \le CAP_{t,p,i_a}^{nG} + CAP_{t,p,i_d}^{eG} \le G_{t,p,i}^{\max} \tag{38}$$

On the other hand, the storage margin for excess generation capacity is expressed as:

$$\begin{aligned} &\left(1+RM_t^{\min}\right) \sum_{p \in P} \sum_{b \in B} D_{\text{peak}} \le \left(1 \pm CF^r\right) \\ &\left(\sum_{i \in I} \sum_{a \in A} CAP_{t,i_a}^{nG} + \sum_{i \in I} \sum_{d \in D} CAP_{t,i_d}^{eG} \right) \le \left(1+RM_t^{\max}\right) \sum_{p \in P} \sum_{b \in B} D_{\text{peak}} \end{aligned} \tag{39}$$

$$\left(1-CF^{g}\right)EENS_{t} \le EENS^{\max} \quad (40)$$

where in Equs. (39) and (40), RM_t^{min} and RM_t^{max} are the restrictions of the reservation margin, respectively; D_{peak} is the average peak demand, and CF^r is a corrective actions associated with the generation reserve margin [15].

E. *Fifth Level Planning*

At this level, transmission expansion planning considering transmission switching as low-cost corrective actions is proposed. In Equ. (41), ${IC_t}^{TL}$ and ${IC_t}^{TS}$ are the cost of investing in candidate transmission lines and transmission switching, and CC_{total} is the congestion cost [15].

$$\min_{uv \in UV} of: OF = \left[\sum_{t\in T}\frac{{IC_t}^{TL}}{(1+d)^{t-t_0}}+\sum_{t\in T}\frac{{IC_t}^{TS}}{(1+d)^{t-t_0}}+\sum_{t\in T}\frac{CC_{total}}{(1+d)^{t-t_0}}\right] \quad (41)$$

In Equ. (42), the capital cost of installed transmission candidate lines is the product of the capital cost of the installed transmission candidate lines of each corridor by the number of lines augmented in each corridor, and expressed by [31]:

$${IC_t}^{TL} = \sum_{TS\in L} IC_{t,tl}^{TL}.\,TL \quad :\forall tl \in TL \quad (42)$$

where TL is refer to the transmission lines augmented in the corridor, and $IC_{t,tl}^{TL}$ is the capital cost of a candidate installed transmission lines in the corridor [31].

On the other hand, In Equ. (43), the capital cost of the newly installed transmission lines of each corridor is calculated as the product of the transmission line construction cost by the active power flow of each corridor and the length of the corridor, as given:

$$IC_{t,tl}^{TL} = FCC_{TL} L_{tl} F_{t,tl} \quad (43)$$

where FCC_{TL} is the construction cost for a transmission; L_{tl} is the length of the corridor; $F_{t,tl}$ is active power flow in the corridor. The capital cost of a candidate installed transmission switching is the product of the capital cost of the candidate installed transmission switching in each corridor by the transmission switching augmented in corridor and expressed using Equ. (44) [15]:

$${IC_t}^{TS} = \sum_{TS\in L} {IC_{t,tl}}^{TL} TS \quad :\forall tl \in TL \quad (44)$$

where TS is the transmission switches augmented in the corridor. The capital cost of the candidate installed transmission switching is expressed in Equ. (45):

$$IC_{t,tl}^{TS} = FCC_{TS} \cdot F_{t,tl} \quad (45)$$

where FCC_{TS} is the fundamental construction cost for a transmission switch.

1) Fifth Level Planning Constraints

In this section, the limitations associated with transmission expansion planning are presented using Equs. (46)-(49). The maximum number of transmission lines which is augmented is explained in Equ. (46). Equ. (47) demonstrates the maximum transmission switching that can be augmented in each corridor and in each period. Equs. (48) and (49) express the total budget constraints available for the transmission network and switching device, respectively [31].

$$TL \le TL^{\max} \quad (46)$$

$$TS \le TS^{\max} \quad (47)$$

$${IC_{t,tl}}^{TL} + {IC_{t,tl}}^{TS} \le \Phi_t \quad (48)$$

$${IC_{t,tl}}^{TL} + {IC_{t,tl}}^{TS} \le \Phi \quad (49)$$

The weight of each disaster scenario *w* in *r* with severity *n* for ruining the GenCos and TLs in Equs. (50) and (51), respectively [15]:

$$\psi_{t,p,i}(w) = \frac{\chi_{t,p}^{r(n):w(h)}}{\varphi_{t,p,i}^{r(n):w(h)}} \Big/ \sum_{\substack{w'\in W \\ w'\neq w}} \frac{\chi_{t,p}^{r(n):w'(h)}}{\varphi_{t,p,i}^{r(n):w'(h)}} \quad (50)$$

$$\psi_{t,p,tl}(w) = \frac{\chi_{t,p}^{r(n):w(h)}}{\varphi_{t,p,tl}} \Big/ \sum_{\substack{w'\in W \\ w'\neq w}} \frac{\chi_{t,p}^{r(n):w'(h)}}{\varphi_{t,p,tl}^{r(n):w'(h)}} \quad (51)$$

By the same token, the weight of each disaster scenario *q* in *c* with severity *m* for ruining the GenCos and TLs are expressed in Equs. (52) and (53), respectively [15].

$$\psi_i(q) = \frac{\chi_{t,p}^{c(m):q(k)}}{\varphi_{t,p,i}} \Big/ \sum_{\substack{q'\in q \\ q'\neq q}} \frac{\chi_{t,p}^{c(m):q'(k)}}{\varphi_{t,p,i}^{c(m):q'(k)}} \quad (52)$$

$$\psi_{t,p,tl}(q) = \frac{\chi_{t,p}^{c(m):q(k)}}{\varphi_{t,p,tl}} \Big/ \sum_{\substack{q'\in q \\ q'\neq q}} \frac{\chi_{t,p}^{c(m):q'(k)}}{\varphi_{t,p,tl}^{c(m):q'(k)}} \quad (53)$$

III. Solution Methodology

In this paper, in order to solve the nonlinear problem, the differential evolution algorithm (DEA) and the symphony orchestra search algorithm (SOSA) are used. The meta-heuristic methods have attracted attention due to simplicity, resilience, not requiring differentiation, and skipping local optima. In this paper, the meta-heuristic DE algorithm is used, which can be classified as evolutionary algorithms. This algorithm employs a differential operator to generate new solutions, it is population-based, its behavior is stochastic, and starts by a set of suggested responses, and tries to achieve a better result in a set of sequential iterations. The unique method of this algorithm for generating new solutions makes it more efficient compared to other optimization algorithms. Since correct selection of the optimal location prevents capital and time loss, this issue should be considered in particular. Optimization is to satisfy min and max destinations of the objective function by formulating and solving it in terms of cost, efficiency, profit and etc. In the DE algorithm, all members of a population have an equal chance to be selected as a parent. The Details were described in [36]. In the first step, the initial information of the proposed hub, like parameters and inputs are introduced, and the gas used by the boiler and CHP

are allocated based on the algorithm populations at t=1 (Fig. 2).

Step 1: Enter the network load data.

Step 2: Select the required parameters.

Step 3: Initialize the memory of the optimization algorithm of interest.

Step 4: Repeat the optimization algorithm.

Step 5: At time t = 1, Add all selected candidate GTEP for each replacement.

Step 6: Create a new solution vector.

Step 7: Set the planning patterns to p = 1.

Step 8: Execute the first level of this algorithm (includes the corrective actions).

Step 9: Run the second level of this algorithm (includes adjusting the event counter, intensity and number of scenarios for earthquake prone regions, which is saved after identifying the vulnerable levels), solve the catastrophic event problems for earthquake-prone regions Then save the vulnerable levels specified after execution. Finally, save the weights of destructive scenarios, save the worst scenario).

Step 10: Execute the third and fourth levels. Then save generation expansion plans, check reserve margins, and EENS, calculate and send the defects of each constraint, save the final generation expansion plan, and implement. Determine the capital cost of the transmission lines, the capital cost of the transmission switching, and congestion cost, and save the final transmission expansion plan

Step 11: $t = t + 1$, If $t<T$ go to step 5.

Step 12: Find the current objective function.

Step 13: Is the new solution better than the solution stored in memory?

Step 14: Save and update the new solution in memory.

Step 15: The successful solution is finished.

Modeling by the SOSA of the problem is as follows:

First, parameters and initial values are added to the algorithm.

Then, in the next step, the initial values are analyzed and sorted. The next step is to improve the problem. For the mentioned problem, it is done as follows. First, all network and energy hub information is entered into the algorithm. Then, the optimal state of the energy hub is calculated and stored in the memory of the algorithm. The next step is to implement the 5 mentioned steps.

The graphical representation of SOSA parameters is shown in Fig. 3.

IV. Results and Discussions

The proposed model was implemented by a PC with a Intel Core i5 processor and 8 GB RAM. Fig. 4 shows the network diagram on Iran's map. In 5-year planning horizon a five-level expansion plan has been used to maximize social welfare and considering corrective actions and switching capability to heighten resilience and minimize costs. The candidate new substations and transmission corridors are represented with dashed circles and lines, respectively. With extensive studies in this area, the impact of renewables such as wind turbines are used to meet part of consumer demand in the proposed hub [37]-[38]-[39]- [40]. Since the EH can partially operate based on the capacity, this paper evaluates the proposed hub based on changes in its location. Thus, the best location for the hub by implementing wind turbine is demonstrated. The proposed method leads to cost-effective results Earthquake prone regions and attack prone are divided into West, Southeast, North, Northeast and South, which are represented in cream, blue, yellow, purple, and pink. In this paper, three possible intensity of earthquake and attack which are including medium, relatively severe, and severe. List of attacks and threats are provided in [30], [41]. Also, IC^{EENS}, CF^{g}, and CF^{r} are 250 MWh, 25MW, and 0.001, respectively. The interest rates were set at 10%. The system information is given in [36]. The meteorological data is selected based on the International Institute of Seismology and Earthquake Engineering website [42]. In this paper, in order to evaluate the effectiveness of the proposed CGTEP, two simulations with and without considering ESs and corrective actions in a 52-bus 400 kV network in Iran are defined and applied. Also, this study is compared with the previous study that the EH was ignored [15]. The five-level CGTEP by applying the proposed hub with and without of storage devices without considering and evaluating the earthquake-induced events in the first to third scales of earthquake are shown in Tables 2 and 3. Similarly, Tables 4 and 5 shows the results of earthquake-induces events, aiming to heighten resilience. Results of Table 3 and 5 by applying the proposed EH in the absence/presence of ESs show that by applying short and long-term corrective actions, the investment costs are reduced and the profit is increased, significantly. Also comparing Tables 3 and 5 by applying the proposed EH in the absence/presence of electrical and thermal ESs with [15] (without proposed hub) shows the cost reduction. An in-depth look and comparison of the results proposed EH in Table 3 and 5 with absence ESs and comparing it with the results in [15], reduction of transmission switching capital costs (IC^{TS}) in three scales by 73.41%, 76.08%, and 0.66% is obvious. On the other hand, show a reduction of 5.91%, 1.08%, and 1.27% in the capital cost of the transmission lines (IC^{TL}), compared to [15]. The congestion cost (CC_{total}) is also measured in three scales is reduced 1.33% ، 1%, and 3.44% by applying the proposed hub to the levels compared to the study conducted in [15]. In this study, the expected profit of the generation units (EB^{GU}) has increased 3.25%, 1.5%, and 1.56%. To this end, the capital cost of generation units (IC^{nGU}) has reduced 9.93%, 11.33%, and 9.71%. The payment capacity paid to generation units GenCos (CAP^{GU}) so has reduced by 1.5%, 2.02%, and 2.6%, compared to [15]. Similarly to, the comparison of the results proposed EH in Table 3 and 5 with presence ESs and

comparing it with the results in [15], reduction of transmission switching capital costs (IC^{TS}) in all three scales by 73.31%, 2.43%, and 0.67% is obvious. On the other hand, show a reduction of 5.57%, 3.15%, and 3.58% in the capital cost of the transmission lines (IC^{TL}). The congestion cost (CC_{total}) is also measured in three scales considering short and long-term reactions, which is reduced 1.27% ,2.83 %, and 6.91%. In this study, the expected profit of the generation units (EB^{GU}) has increased 1%, 4.64%, and 3.64%. To this end, the capital cost of all generation units (IC^{nGU} has reduced 12.6%, 14.76%, and 14.93%. The payment capacity paid to all generation units GenCos (CAP^{GU}) so has reduced by 1.7%, 3.43%, and 6.7%, which has reduced by 1.6%, 3%, and 7.3% compared to [15]. As can be seen from the results, the implementation of short and long-term reactions also the presence of the proposed hub with ESs in CGTEP is effective to heighten resilience, minimize the costs and maximize profit. In additionally, an in-depth look and comparison of the results presented in Table 3 by ignoring corrective actions and absence/presence ESs show that the capital costs of transmission switches (IC^{TS})

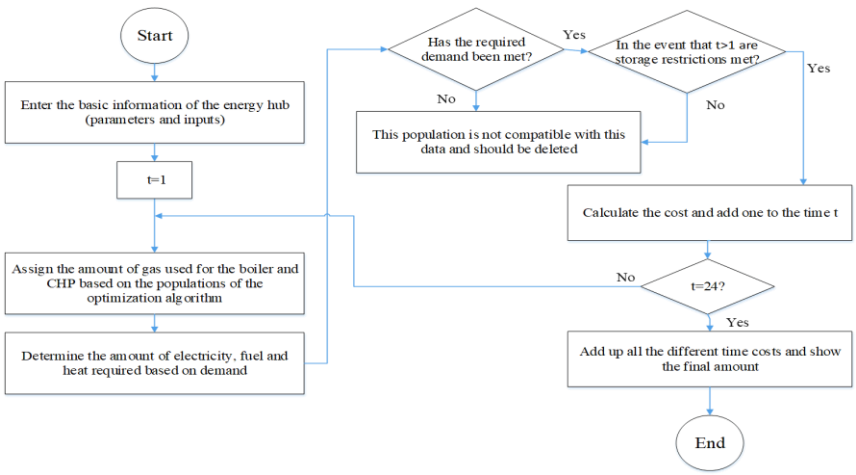

Fig. 2. The proposed energy hub optimization.

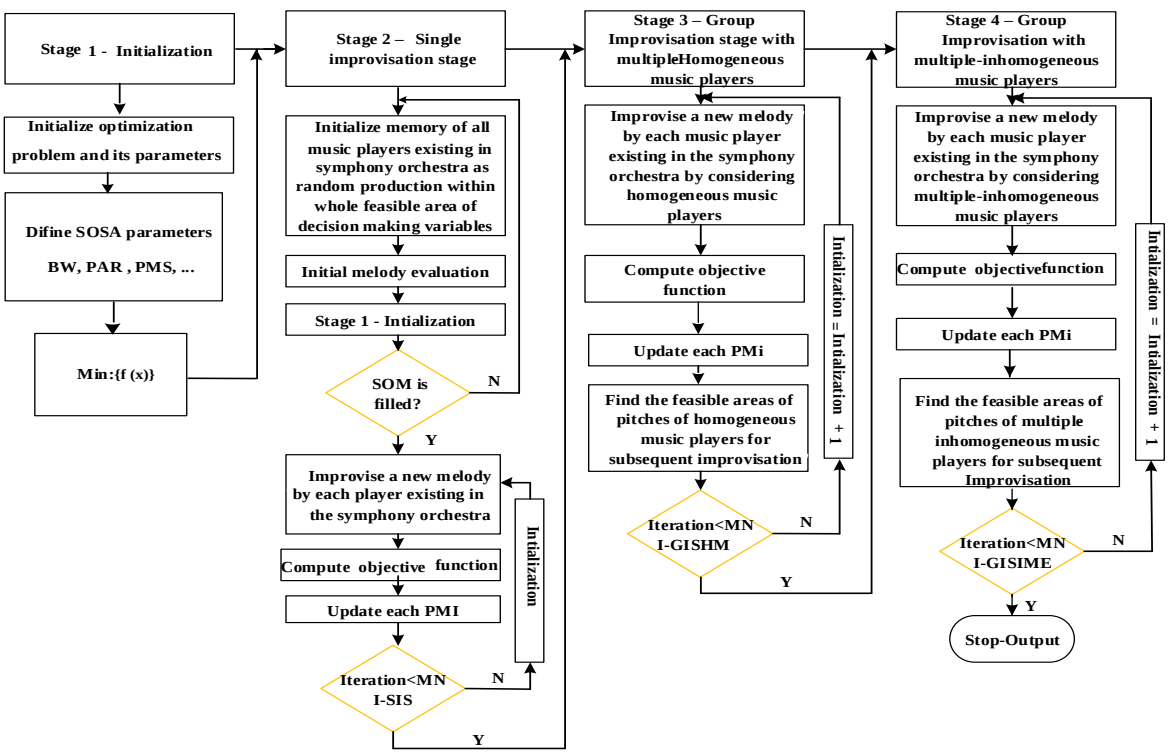

Fig. 3. The graphical representation of SOSA parameters

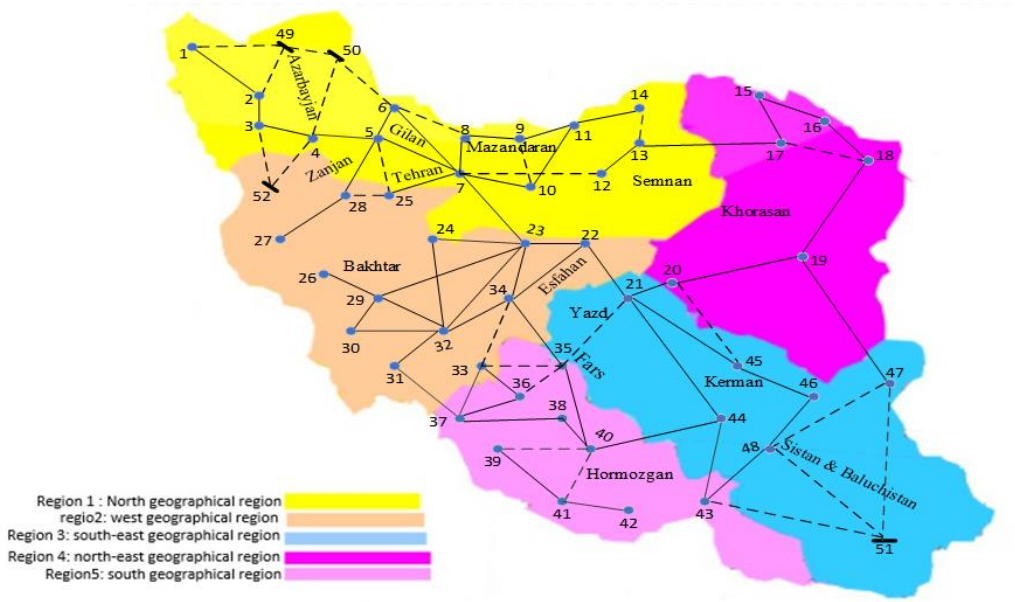

Fig. 4. 400-kV test system with 52 buses in Iran

Considering three scales of the events are reduced by 3.42%, 3.43%, and 1.66%, respectively. On the other hand, a reduction of 2.38%,0.75%, and 5.05%, in the capital cost of the transmission lines (IC^{TL}). The congestion cost (CC_{total}) is reduced by 1.75% ، 2.06%, and 0.41%. In this study, the expected profit of the generation units (EB^{GU}) has increased 0.44%, 3.56%, and 1.79%. The capital cost of all generation units (IC^{nGU}) has reduced 3.57%, 5.75%, and 5.77%. The payment capacity paid to all generation units GenCos (CAP^{GU}) so has reduced by 1.25%, 1.77%, and 3.53%. Similarly to, the comparison of the results presented in Table 5 by considering corrective actions and absence/presence ESs show that the investment costs of all transmission switches (IC^{TS}) considering the three scales of the events are reduced by 1.47%, 0.97% , and 1.17%, respectively. On the other hand, a reduction of 2.95%, 1.71%, and 1.57%, in the investment cost of the transmission lines (IC^{TL}) . The congestion cost (CC_{total}) is reduced by 1.65% ، 5.28%, and 4%. In this study, the expected profit of the generation units (EB^{GU}) has increased 3.5%, 0.48%, and 0.17%. The investment cost of generation units (IC^{nGU}) has reduced 0.55%, 1.86%, and 0.01%. The payment capacity paid to all generation units GenCos (CAP^{GU}) so has reduced by 2.48%, 0.09%, and 1.%. In additionally, depth look and comparison of the results presented in Table 3 and 5 by considering corrective actions and absence ESs show that the capital costs of transmission switches (IC^{TS}) considering three scales of the events are reduced by 91.69%, 88.97%, and 8.81%, respectively. On the other hand, a reduction of 40.87%, 39.21%, and 36.9%, in the capital cost of the transmission lines (IC^{TL}). The congestion cost (CC_{total}) is reduced by 33.61% ، 43.06%, and 47.3%. In this study, the expected profit of the generation units (EB^{GU}) has increased 1.85%, 6.83%, and 7.65%. The capital cost of generation units (IC^{nGU}) has reduced 30.95%, 16.94%, and 15.08%. The payment capacity paid to generation units GenCos (CAP^{GU}) by so has reduced 16.62%, 14.48%, and 13.01%. Similarly to, the comparison of the results presented in Table 5 by considering corrective actions and presence ESs show that the capital costs of transmission switches (IC^{TS}) considering three scales of the events are reduced by 91.52%, 10.46% , and 8.82%, respectively. On the other hand, a reduction of 41.21%,43.44%, and 34.59%, in the capital cost of the transmission lines (IC^{TL}). The congestion cost (CC_{total}) is reduced by 33.55% ، 44.93%, and 50.77%. In this study, the expected profit of the generation units (EB^{GU}) has increased 5.03%, 3.66%, and 5.57%. The capital cost of generation units has reduced 28.28%, 13.51%, and 9.86%. The payment capacity paid generation units GenCos (CAP^{GU}) so has reduced by 16.78%, 15.89%, and 17.06%. According to the results, for all three scales by applying the proposed hub and corrective ctions the expected profit tends to increase, and the installation cost tends to decrease that can improved the grid resilience. The Fig. 5(a) shows the number of generation units, transmission lines and transmission switching with the presence of the proposed EH and without considering short and long-term corrective actions in three scales. In the first scale, 19 generation units, 34 transmission lines, and 4 transmission switches are needed. In the second scale, 34 generation units, 38 transmission lines, and 41 transmission switches are needed. In third scale, 4 generation units, 4 transmission lines and 6 transmission switches are needed. Therefore, the number of elements is reduced compared to [15]. The Fig. 5(b) shows the number of generation units, transmission lines and transmission switching with the

presence of the proposed EH together with considering short and long-term corrective actions in three scales. In the first scale, 14 generation units, 15 transmission lines, and 21 transmission switches are needed. In the second scale, 18 generation units, 22 transmission lines, and 32 transmission switches are needed. In third scale, 3 generation units, 4 transmission lines and 5 transmission switches are needed. Thus, the number of elements is reduced compared to [15]. The Fig. 5(c) shows that with the proposed method, will have a significant reduction in IC^{TL}. The amount of the curtailed load in 400-kV power grid in two case (considering & ignoring corrective actions) in three scales are shown in Figs. 6(a-c).

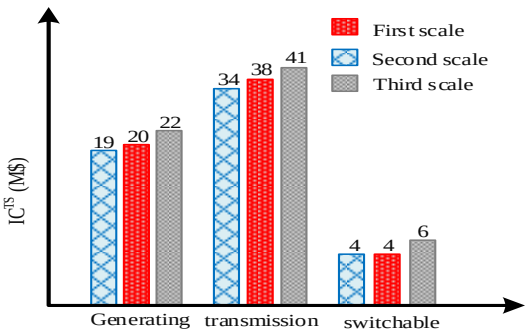

(a): Without considering short and long-term corrective actions

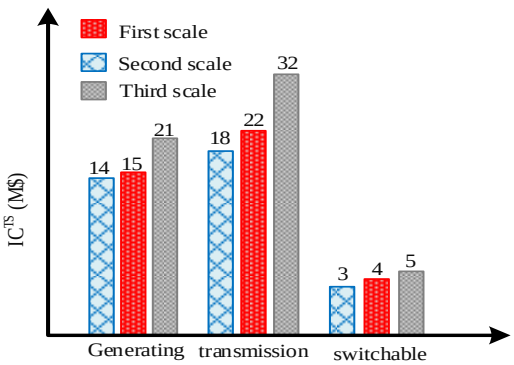

(b): With considering short and long-term corrective actions.

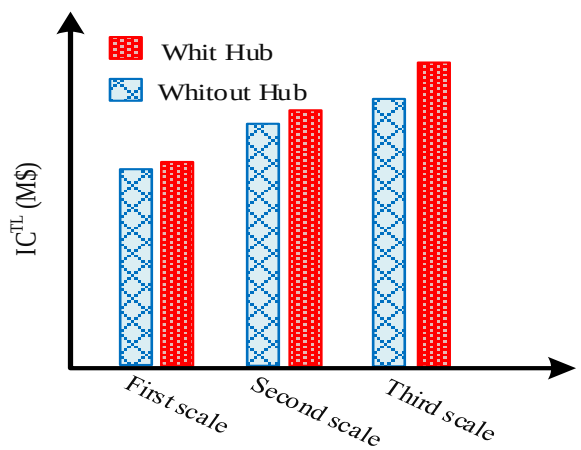

(c): Without & with considering proposed EH.

Fig. 5. Comparison of the number of elements and capital costs of transmission lines in different scales.

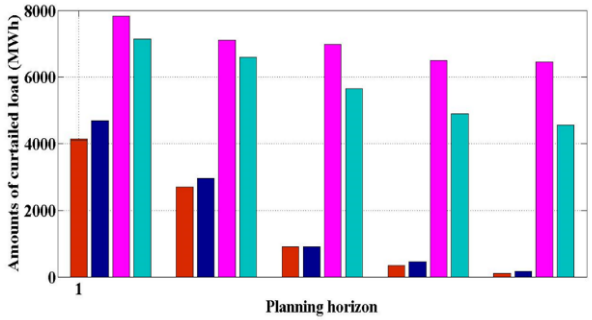

(a): First scale.

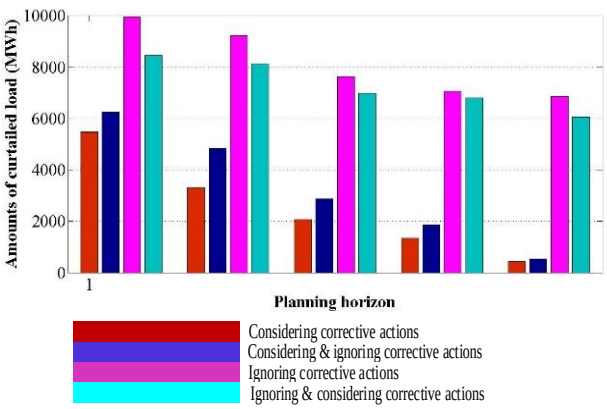

(b) second scale

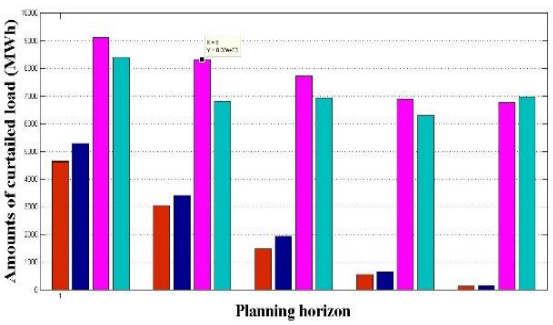

(c): third scale.

Fig. 6. The amounts of the curtailed load in different scales

TABLE 2
THE EXPANSION PLANS FOR THREE SCALES OF EARTHQUAKE BY IGNORING T CORRECTIVE ACTIONS

Planning Periods	Generating units	Transmission lines	Switchable transmission lines	Generating units	Transmission lines	Switchable transmission lines	Generating units	Transmission lines	Switchable transmission lines
period 1	9, C 17, I 43, I	(1-2), I (1-49), C (11-14), I (21-45), I (23-32), I (29-32), I (39-40), C	(35-40), I	14, C 20, C 21, I	(13-14), C (21-22), I (35-40), I (38-40), I (40-41), C (43-48), I (47-48), C	(23-34), I	5, C 9, C 11, I 18, C 48, I	(4-52), C (7-12), C (13-14), C (19-20), I (21-35), C (22-23), I (22-34), I (24-32), I (46-48), I	(31-32), I
period 2	2, I 11, I 44, C 48, I	(5-25), C (16-18), I (21-35), C (23-29), I (29-32), I (30-32), I (41-42), I		5, C 15, I 21, I 33, C 50, C	(7-8), I (10-11), I (17-18), C (23-24), I (31-32), I (35-36), C (37-38), I (46-48), I	(33-37), I	7, I 30, I 50, C 21, I 17, I	(4-50), C (7-10), I (7-23), I (11-14), I (15-17), I (27-28), I (33-34), C (8-9), I (43-48), I	(23-29), I
period 3	19, I 22, I 33, C 42, C 48, I	(4-5), I (23-24), I (31-37) , I (33-37), I (40-41), C (43-44), I (47-51), C	(38-40), I	6, I 16, I 36, C 39, C 43, I	(4-50), C (13-14), C (15-16), I (22-34), I (29-30), I (33-36), I (37-38), I (45-46), I	(18-19), I	20, C 23, C 34, I 48, I	(1-49), C (22-23), I (23-34), I (33-37), I (38-40), I (40-41), C (45-46), I (47-48), C	(31-37), I
period 4	7, I 20, C 32, I 37, I	(3-52), C (5-25), C (9-10), C (22-23), I (40-44), I (41-42), I (9-11), I	(21-44), I	1, I 2, I 20, C 50, C	(1-2), I (5-7), I (5-25), C (8-9), I (10-11), I (21-45), I (32-34), I (45-46), I	(7-25), I	25, C 36, C 39, C 48, I 50, C	(5-6), I (5-28), I (6 -50), C (7-25), I (18-19), I (21-35), C (23-34), I (29-30), I (41-42), I	(12-13), I
period 5	7, I 44, C 47, I	(3-4), I (5-7), I (9 -11), I (13-17), I (29-32), I (34-35), I (49-50), C	(33-37), I	20, C 30, I 42, C 44, C	(6-7), I (8-9), I (13-14), C (24-32), I (31-32), I (34-35), I (39-41), I (43-51), C	(7-23), I	19, I 30, I 51, C 33, C	(6-7), I (7-23), I (15-17), I (18-19), I (20-45), C (21-22), I (25-28), C (33-37), I	(9-11), I (5-7), I

TABLE 3
THE OBTAINED VALUES FOR THREE SCALES OF EARTHQUAKE BY IGNORING CORRECTIVE ACTIONS WITH PROPOSED EH

No.	Objective function	First scale without electrical and thermal storage	First scale with electrical and thermal storage	Second scale without electrical and thermal storage	Second scale with electrical and thermal storage	Third scale without electrical and thermal storage	Third scale with electrical and thermal storage
1	IC^{TL}	893.571	872.241	1105.894	1097.526	1368.182	1299.042
2	IC^{TS}	890.837	860.362	108.628	104.901	131.257	129.727
3	CC_{total}	38.0289	37.362	36.858	36.098	31.087	30.958
4	EB^{GU}	59.972	60.241	68.388	70.827	87.684	89.261
5	IC^{nGU}	450.382	431.274	506.378	477.261	637.056	600.271
6	CAP^{GU}	33.502	33.921	38.574	39.258	43.158	44.685
7	Total number	19 Generating 35 Transmission 4 Switchable	19 Generating 34 Transmission 4 Switchable	21 Generating 39 Transmission 5 Switchable	20 Generating 38 Transmission 4 Switchable	23 Generating 43 Transmission 6 Switchable	22 Generating 41 Transmission 6 Switchable

TABLE 4
THE EXPANSION PLANS FOR THREE SCALES OF EARTHQUAKE BY CONSIDERING CORRECTIVE ACTIONS

Planning Periods	Generating units	Transmission lines	Switchable transmission lines	Generating units	Transmission lines	Switchable transmission lines	Generating units	Transmission lines	Switchable transmission lines
period 1	2, I 19, I 36, C	(7-8), I (12-13), I (22-23), I (23-24), I		11, I 15, I 20, C	(8- 9), I (13-14), C (16-18), I (19-47), I (21-35), C	(21-45), I	6, I 13, C 15, I	(4-52), C (6-7), I (7-12), C (7-25), I (21-22), I (23-29), I (34-35), I (46-48), I	(24-32), I
period 2	26, C 30, I 32, I 37, I	(3-4), I (4-5), I (5-25), C	(20-21), I	11, I 13, C 46, C	(2-3), I (5-7), I (12-13), I (20-21), I (23-34), I (30-32), I	(21-44), I	4, I 14, C 26, C 43, I	(18-19), I (21-44), I (21-45), I (23-29), I (23-32), I (27-28), I	(8-9), I (12-13), I
period 3	21, I 28, I	(5-28), I (8-9), I (12-13), I	(21-45), I	15, I 37, I 41, I 48, I	(2-49), C (3-4), I (13-14), C (33-37), I		3, I 32, I 36, C 45, I	(5-25), C (10-11), I (15-17), I (19-47), I (26-29), I	
period 4	16, I 25, C 30, I	(4-50), C (7-23), I (15-17), I (18-19), I		10, C 17, I 26, C	(3-4), I (4-5), I (4-50), C (9-10), C (11-14), I	(33-35), C	6, I 7, I 27, I 35, C 44, C	(4-5), I (6-8), C (9-10), C (22-23), I (22-34), I (33-35), C (33-36), I	(11-14), I
period 5	27, I 28, I	(36-37), I (37-38), I (40-41), C (48-51), C	(19-47), I	1, I 5, C	(5-25), C (11-14), I (17-18), C (29-32), I	(23-32), I	8, C 15, I 34, I 38, I	(4-5), I (4-50), C (5-25), C (15-17), I (21-44), I (29-32), I (37-38), I	(33-37), I

TABLE 5
THE OBTAINED VALUES FOR THREE SCALES OF EARTHQUAKE BY CONSIDERING CORRECTIVE ACTIONS WITH PROPOSED EH

No	Objective function	First scale without electrical and thermal storage	First scale with electrical and thermal storage	Second scale without electrical and thermal storage	Second scale with electrical and thermal storage	Third scale without electrical and thermal storage	Third scale with electrical and thermal storage
1	IC^{TL}	528.357	512.73	672.252	660.762	863.293	849.701
2	IC^{TS}	73.985	72.893	94.852	93.927	119.682	118.274
3	CC_{total}	25.244	24.826	20.985	19.876	16.381	15.725
4	EB^{GU}	61.083	63.275	73.065	73.421	94.398	94.2376
5	IC^{nGU}	310.982	309.271	420.583	412.749	540.987	541.071
6	CAP^{GU}	27.933	28.628	32.987	33.017	37.542	37.061
7	Total number	14 Generating 18 Transmission 3 Switchable	14 Generating 18 Transmission 3 Switchable	15 Generating 24 Transmission 4 Switchable	15 Generating 22 Transmission 4 Switchable	20 Generating 33 Transmission 5 Switchable	21 Generating 32 Transmission 5 Switchable

V. Conclusions

Considering a dynamic approach enables us to make expansion decisions at different points in time, which increases the resilience of the decision-maker and reduces the investment budget required at the beginning of the planning horizon. Considering the necessity of resilience studies, our purpose is to heighten resilience of power systems by applying the proposed EH using wind turbine, with and without of ESs and employing DE algorithm and SOSA, which can be used for different optimization problems. In this paper, a nonlinear five-level CGTEP approach in large scale is proposed to minimize the capital costs and achieve the optimal solution. Several levels of simultaneous expansion planning have been implemented in this study. At the first level, system Uncertainties were modeled by taking into account the thermal energy market, a DR program, and the use of wind turbines in the proposed hub, with the goal of increasing resilience while minimizing input energy transfer costs and operating costs. The second level depicts the system operator's corrective actions following the accident to reconfigure the network. Third level earthquake events are modeled and evaluated as unknown events. At the fourth level, planning for generation planning is done with the goal of increasing resilience. The fifth level of transmission expansion planning focuses on resilience, and the ability to switch transmission lines is viewed as a low-cost correction factor. In this paper, the costs and modeling uncertainties in the optimal expansion planning in the presence of the proposed hub play an essential role in heightening resilience. The line switching maneuvers, short-term and long-term corrective actions as the resilient sources are considered to increase the power system resilience in response to variable changes of the system demand. This study has presented an optimal strategy to minimize load curtailment. On the other hand, the findings of this study compared with the previous study that the EH was ignored. The ultimate goal is to maintain system performance after events such that the system adapts itself with the events after absorbing the disruptions and reduce the consequences by fast recovery. The numerical simulations indicate the effectiveness of the proposed strategy for heightening resilience. DR programs and storage systems are known as two effective approaches to reduce the impact of uncertainties. The presence of an EH on the bus, results in changes in productive power which is the first impact on the issue. As demonstrated by the results, implementing short and long-term reactions in conjunction with concurrent generation and transmission expansion planning has been effective in strengthening resilience, minimizing costs, and increasing profits.

REFERENCES

[1] X. Luo and Y. Liu, "A multiple-coalition-based energy trading scheme of hierarchical integrated energy systems," *Sustainable Cities and Society*, vol. 64, p. 102518, 2021.

[2] S. Rahgozar, A. Z. G. Seyyedi, and P. Siano, "A resilience-oriented planning of energy hub by considering demand response program and energy storage systems," *Journal of Energy Storage*, vol. 52, p. 104841, 2022.

[3] R. Yan, T. K. Saha, F. Bai, and H. Gu, "The anatomy of the 2016 South Australia blackout: A catastrophic event in a high renewable network," *IEEE Transactions on Power Systems*, vol. 33, no. 5, pp. 5374-5388, 2018.

[4] X. Zhang, S. Mahadevan, S. Sankararaman, and K. Goebel, "Resilience-based network design under uncertainty," *Reliability Engineering & System Safety*, vol. 169, pp. 364-379, 2018.

[5] K. Ramirez-Meyers, W. N. Mann, T. Deetjen, S. Johnson, J. Rhodes, and M. Webber, "How different power plant types contribute to electric grid reliability, resilience, and vulnerability: a comparative analytical framework," *Progress in Energy*, vol. 3, no. 3, p. 033001, 2021.

[6] S. Lumbreras and A. Ramos, "The new challenges to transmission expansion planning. Survey of recent practice and literature review," *Electric Power Systems Research*, vol. 134, pp. 19-29, 2016.

[7] A. Hussain, V. H. Bui, and H. M. Kim, "Optimal operation of hybrid microgrids for enhancing resiliency considering feasible islanding and survivability," *IET Renewable Power Generation*, vol. 11, no. 6, pp. 846-857, 2017.

[8] G. Jayadev, B. D. Leibowicz, and E. Kutanoglu, "US electricity infrastructure of the future: Generation and transmission pathways through 2050," *Applied energy*, vol. 260, p. 114267, 2020.

[9] S. M. Mohseni-Bonab, I. Kamwa, A. Rabiee, and C. Chung, "Stochastic optimal transmission Switching: A novel approach to enhance power grid security margins through

vulnerability mitigation under renewables uncertainties," *Applied Energy*, vol. 305, p. 117851, 2022.
[10] C. A. Sima, M. O. Popescu, C. L. Popescu, M. Alexandru, and G. Lazaroiu, "Increasing RESS share using generation and transmission expansion planning-stochastic approach," in *2019 11th International Symposium on Advanced Topics in Electrical Engineering (ATEE)*, 2019: IEEE, pp. 1-6.
[11] S. A. Eghbali Khob, M. Moazzami, and R. Hemmati, "Advanced model for joint generation and transmission expansion planning including reactive power and security constraints of the network integrated with wind turbine," *International Transactions on Electrical Energy Systems*, vol. 29, no. 4, p. e2799, 2019.
[12] X. Yang, Z. Chen, X. Huang, R. Li, S. Xu, and C. Yang, "Robust capacity optimization methods for integrated energy systems considering demand response and thermal comfort," *Energy*, vol. 221, p. 119727, 2021.
[13] A. Ahmarinejad, "A multi-objective optimization framework for dynamic planning of energy hub considering integrated demand response program," *Sustainable Cities and Society*, vol. 74, p. 103136, 2021.
[14] T. Xu, C. Shao, M. Shahidehpour, and X. Wang, "Coordinated Planning Strategies of Power Systems and Energy Transportation Networks for Resilience Enhancement," *IEEE Transactions on Sustainable Energy*, 2022.
[15] M. Shivaie, M. Kiani-Moghaddam, and P. D. Weinsier, "A vulnerability-constrained quad-level model for coordination of generation and transmission expansion planning under seismic-and terrorist-induced events," *International Journal of Electrical Power & Energy Systems*, vol. 120, p. 105958, 2020.
[16] W. Gan *et al.*, "A tri-level planning approach to resilient expansion and hardening of coupled power distribution and transportation systems," *IEEE Transactions on Power Systems*, vol. 37, no. 2, pp. 1495-1507, 2021.
[17] Y.-P. Fang, C. Fang, E. Zio, and M. Xie, "Resilient critical infrastructure planning under disruptions considering recovery scheduling," *IEEE Transactions on Engineering Management*, vol. 68, no. 2, pp. 452-466, 2019.
[18] Y. Wang, A. O. Rousis, and G. Strbac, "A Three-Level Planning Model for Optimal Sizing of Networked Microgrids Considering a Trade-Off Between Resilience and Cost," *IEEE Transactions on Power Systems*, vol. 36, no. 6, pp. 5657-5669, 2021.
[19] K. Yurtseven and E. Karatepe, "Influence of inherent characteristic of PV plants in risk-based stochastic dynamic substation expansion planning under MILP framework," *IEEE Transactions on Power Systems*, vol. 37, no. 1, pp. 750-763, 2021.
[20] C. Guo, C. Ye, Y. Ding, and P. Wang, "A multi-state model for transmission system resilience enhancement against short-circuit faults caused by extreme weather events," *IEEE Transactions on Power Delivery*, vol. 36, no. 4, pp. 2374-2385, 2020.
[21] Y.-K. Wu, Y.-C. Chen, H.-L. Chang, and J.-S. Hong, "The effect of decision analysis on power system resilience and economic value during a severe weather event," *IEEE Transactions on Industry Applications*, vol. 58, no. 2, pp. 1685-1695, 2022.
[22] Y.-K. Wu, Y.-C. Wu, H.-L. Chang, and J.-S. Hong, "Using Extreme Wind-Speed Probabilistic Forecasts to Optimize Unit Scheduling Decision," *IEEE Transactions on Sustainable Energy*, vol. 13, no. 2, pp. 818-829, 2021.
[23] T. Hussain, S. Suryanarayanan, T. M. Hansen, and S. S. Alam, "A Fast and Scalable Transmission Switching Algorithm for Boosting Resilience of Electric Grids Impacted by Extreme Weather Events," *IEEE Access*, 2022.
[24] D. N. Trakas and N. D. Hatziargyriou, "Strengthening transmission system resilience against extreme weather events by undergrounding selected lines," *IEEE Transactions on Power Systems*, vol. 37, no. 4, pp. 2808-2820, 2021.
[25] M. Abdelmalak and M. Benidris, "Enhancing power system operational resilience against wildfires," *IEEE Transactions on Industry Applications*, vol. 58, no. 2, pp. 1611-1621, 2022.
[26] M. Abdelmalak and M. Benidris, "Proactive Generation Redispatch to Enhance Power System Resilience During Hurricanes Considering Unavailability of Renewable Energy Sources," *IEEE Transactions on Industry Applications*, vol. 58, no. 3, pp. 3044-3053, 2022.
[27] H. Ranjbar, S. H. Hosseini, and H. Zareipour, "Resiliency-oriented planning of transmission systems and distributed energy resources," *IEEE Transactions on Power Systems*, vol. 36, no. 5, pp. 4114-4125, 2021.
[28] Y. Yang, J. C.-H. Peng, C. Ye, Z.-S. Ye, and Y. Ding, "A criterion and stochastic unit commitment towards frequency resilience of power systems," *IEEE transactions on power systems*, vol. 37, no. 1, pp. 640-652, 2021.
[29] K. Garifi, E. S. Johnson, B. Arguello, and B. J. Pierre, "Transmission Grid Resiliency Investment Optimization Model with SOCP Recovery Planning," *IEEE Transactions on Power Systems*, vol. 37, no. 1, pp. 26-37, 2021.
[30] H. Nemati, M. A. Latify, and G. R. Yousefi, "Coordinated generation and transmission expansion planning for a power system under physical deliberate attacks," *International Journal of Electrical Power & Energy Systems*, vol. 96, pp. 208-221, 2018.
[31] Y. Fang and G. Sansavini, "Optimizing power system investments and resilience against attacks," *Reliability Engineering & System Safety*, vol. 159, pp. 161-173, 2017.
[32] M. Zeraati, Z. Aref, and M. A. Latify, "Vulnerability analysis of power systems under physical deliberate attacks considering geographic-cyber interdependence of the power system and communication network," *IEEE Systems Journal*, vol. 12, no. 4, pp. 3181-3190, 2017.
[33] N. M. Tabatabaei, S. N. Ravadanegh, and N. Bizon, *Power Systems Resilience*. Springer, 2018.
[34] M. Vahid-Pakdel, S. Nojavan, B. Mohammadi-Ivatloo, and K. Zare, "Stochastic optimization of energy hub operation with consideration of thermal energy market and demand response," *energy Conversion and Management*, vol. 145, pp. 117-128, 2017.
[35] R. Alvarez, C. Rahmann, R. Palma-Behnke, and P. Estévez, "A novel meta-heuristic model for the multi-year transmission network expansion planning," *International Journal of Electrical Power & Energy Systems*, vol. 107, pp. 523-537, 2019.
[36] M. Kiani-Moghaddam, M. Shivaie, and P. D. Weinsier, *Modern Music-Inspired Optimization Algorithms for Electric Power Systems*. Springer, 2019.
[37] M. T. Askari, M. Z. A. A. Kadir, M. Tahmasebi, and E. Bolandifar, "Modeling optimal long-term investment strategies of hybrid wind-thermal companies in restructured power market," *Journal of Modern Power Systems and Clean Energy*, vol. 7, no. 5, pp. 1267-1279, 2019.
[38] T. Lagos *et al.*, "Identifying optimal portfolios of resilient network investments against natural hazards, with applications to earthquakes," *IEEE Transactions on Power*

Systems, vol. 35, no. 2, pp. 1411-1421, 2019.
[39] M. Askari, M. Ab Kadir, H. Hizam, and J. Jasni, "A new comprehensive model to simulate the restructured power market for seasonal price signals by considering on the wind resources," *Journal of Renewable and Sustainable Energy*, vol. 6, no. 2, p. 023104, 2014.
[40] J. Märkle-Huß, S. Feuerriegel, and D. Neumann, "Cost minimization of large-scale infrastructure for electricity generation and transmission," *Omega*, vol. 96, p. 102071, 2020.
[41] J. Aghaei, N. Amjady, A. Baharvandi, and M.-A. Akbari, "Generation and transmission expansion planning: MILP–based probabilistic model," *IEEE Transactions on Power Systems*, vol. 29, no. 4, pp. 1592-1601, 2014.
[42] M. Hosseini, R. Mirzaei, and S. S. Kourehli, "International Institute of Earthquake Engineering and Seismology."

APPENDIX

Input parameters for simulation.

PARAMETER ADJUSTMENT OF THE OPTIMIZATION

Abbreviation	SOSA parameters	Value
BW	distance bandwidth	$\in R^{(N)} > 0$
MNI - E	Max. number of iterations for second step	MNI - E ≥ 1
MNI - SIS	Max. number of iterations for third step	MNI - SIS ≥ 1
MNI - GISHMG	Max. number of iterations for fourth step	MNI - GISHMG ≥ 1
MNI - GISIME	Max. number of iterations for fifth step	MNI - GISIME ≥ 1
NHMG	Number of decision-making variables	NHMG ≥ 1
PAR	pitch adjusting rate	$0 \leq PAR \leq 1$
$PMCR$	Player memory considering rate	$0 \leq PMCR \leq 1$
PMS	Player memory size	$PMS \geq 1$
PMN	Player memory number	$PMN \geq 1$
MM	Melody memory	-

THE PROPOSED EH PARAMETERS

EH Parameters	Unit	Value	EH Parameters	Unit	Value
η_{GH}^{B}	-	0.85	$\alpha_{H}^{\min}$	-	0.05
P_{E}^{NETMAX}	KW	2000	$\alpha_{H}^{\max}$	-	0.90
P_{G}^{NET}	KW	1800	$\beta_{E}^{\min}$	-	0.05
P_{H}^{NET}	KW	2000	$\beta_{E}^{\max}$	-	0.18
P_{in}^{T}	KW	2000	$\beta_{H}^{\min}$	-	0.05
P_{in}^{CHP}	KW	800	$\beta_{H}^{\max}$	-	0.09
P_{in}^{B}	KW	800	P_{E}^{CAP}	KW	300
α_{E}^{LOSS}	-	0.05	P_{H}^{CAP}	KW	200
α_{H}^{LOSS}	-	0.05	η_{ES}^{ch}	-	0.90
$\alpha_{E}^{\min}$	-	0.05	η_{ES}^{dis}	-	0.90
$\alpha_{E}^{\max}$	-	0.90	η_{HS}^{ch}	-	0.90
v_{out}	m/s	22	v_{r}	m/s	10
Weilbullscale	-	7.87	$\text{LPF}_{\text{down}}^{H}$	-	0.20
η_{GE}^{CHP}	-	0.40	η_{E}^{T}	-	0.90
v_{in}	m/s	4	P_{r}^{WIND}	KW	400
$\text{LPF}_{\text{up}}^{H}$	-	0.20	*Weilbullscale*	-	1.75
π_{E}^{WIND}	Cent/kWh	0	π_{G}^{NET}	Cent/kWh	7.2
π_{H}^{NET}	Cent/kWh	8	π_{E}^{op}	Cent/kWh	0
π_{H}^{op}	Cent/kWh	2	π_{E}^{D}	Cent/kWh	0
π_{H}^{D}	Cent/kWh	0	η_{CONV}^{WIND}	-	0.90
η_{HS}^{dis}	-	0.90	-	-	-

Mahnaz Rezaei was born in Iran in 1988. She received the B.S. degree in electrical engineering from Zahedan Branch Islamic Azad University, Iran in 2010. In 2015, she received the M.Sc. degree in Power electrical engineering, Zahedan Branch Islamic Azad University. She is currently Ph.D candidate in Power Electrical Engineering from Islamic Azad University (Semnan Branch). Her research interests include smart grids, GEP & TEP.

Mohammad Tolou Askari enrolled at University of Applied Science and Technology of Mashhad and obtained his first degree in Bachelor of Power Electrical Engineering in 2005. He continued his education in Master of Power Electrical Engineering in 2008. He received PhD degree in Power electrical engineering (2014) from University Putra Malaysia. Currently, he is Assistant Professor with Islamic Azad University, Semnan, Iran. His research interests include electrical transformers, Smart grids, Micro grids, GEP & TEP, Distribution systems.

Meysam Amirahmadi received the B.Sc. degree in electrical engineering from Guilan University, Rasht, Iran, in 2006 and M.Sc., and Ph.D. degrees in electrical engineering from Semnan University, Semnan, Iran, in 2009 and 2014, respectively. He is currently an Assistant Professor with Islamic Azad University, Semnan, Iran. His research interests include power system planning and operation, electricity markets and smart grids.

Vahid Ghods was born in Iran in 1981. He received the B.S. degree in electronic engineering from Electrical Engineering Faculty, K. N. Toosi University of technology (KNTU), Tehran, Iran, in 2002. In 2005, he received M.Sc. degree in digital electronic from Electrical Engineering Faculty, Semnan University, Semnan, Iran. He received Ph.D. degree in electronic from Electrical Engineering Faculty, Science and research branch, Islamic Azad University, Tehran, Iran, in 2012. He is an associate professor of Engineering Faculty, Semnan branch, Islamic Azad University, Semnan, Iran. His research fields are signal processing, machine vision, image and speech processing and recognition, artificial intelligence and specially OCR.